Experimental Observation of Space-Charge Field Screening of a Relativistic Particle Bunch in Plasma

L. Verra[1,*] M. Galletti,[2,3,4] R. Pompili,[1] A. Biagioni,[1] M. Carillo,[5] A. Cianchi,[2,3,4] L. Crincoli,[1]
A. Curcio,[1] F. Demurtas,[2] G. Di Pirro,[1] V. Lollo,[1] G. Parise,[2] D. Pellegrini,[1] S. Romeo,[1]
G. J. Silvi,[5] F. Villa,[1] and M. Ferrario[1]

[1]INFN Laboratori Nazionali di Frascati, Via Enrico Fermi 54, 00044 Frascati, Italy
[2]University of Rome Tor Vergata, Via Della Ricerca Scientifica 1, 00133 Rome, Italy
[3]INFN Tor Vergata, Via Della Ricerca Scientifica 1, 00133 Rome, Italy
[4]NAST Center, Via Della Ricerca Scientifica 1, 00133 Rome, Italy
[5]University of Rome Sapienza, Piazzale Aldo Moro 5, 00185 Rome, Italy

The space-charge field of a relativistic charged bunch propagating in plasma is screened due to the presence of mobile charge carriers. We experimentally investigate such screening by measuring the effect of dielectric wakefields driven by the bunch in a uncoated dielectric capillary where the plasma is confined. We show that the plasma screens the space-charge field and therefore suppresses the dielectric wakefields when the distance between the bunch and the dielectric surface is much larger than the plasma skin depth. Before full screening is reached, the effects of dielectric and plasma wakefields are present simultaneously.

Introduction.—One of the fundamental properties of plasma is the ability to screen electromagnetic fields, due to the presence of mobile charge carriers (plasma electrons and ions) [1]. The propagation of electromagnetic waves in plasma has been extensively studied [2], especially in the context of plasma generation [3], heating, and confinement [4], requiring complex and dedicated experimental setups [5]. In the case of a relativistic charged particle bunch traveling through a plasma with density n_{PE}, the plasma electrons rapidly move to compensate for the almost purely transverse space-charge field of the bunch. This effect is the cause of phenomena such as plasma wakefields [6,7].

Because of the screening operated by the plasma, the space-charge field of the bunch is exponentially damped with the radial distance r as $E_r \propto e^{-r/\delta}$ [8], where the characteristic length $\delta = c\sqrt{m_e \varepsilon_0 / n_{PE} e^2}$ is the plasma skin depth (c the speed of light, ε_0 the vacuum permittivity, m_e and e the electron rest mass and charge, respectively). Hence, the plasma effectively screens the space-charge field of the bunch when $r \gg \delta$. Despite the physics of the process being well known, no direct experimental evidence of plasma screening has been provided so far for the fields generated by a relativistic charged particle bunch.

In this Letter, we present a noninvasive measurement of plasma screening of the space-charge field of a relativistic electron bunch. We show that screening causes the suppression of dielectric wakefields in an uncoated dielectric capillary, where the plasma is generated, when the distance between the bunch and the capillary surface is much larger than the plasma skin depth. Moreover we observe, for the

first time to our knowledge, the simultaneous effect of dielectric and plasma wakefields, when full plasma screening is not achieved.

A relativistic, charged bunch drives wakefields when its space-charge field interacts with a slow-wave structure or medium with a large index of refraction. Consequently, longitudinal and transverse dielectric wakefields (also known as Cherenkov wakefields) are generated [9–12]. Dielectric transverse wakefields are axis symmetric with respect to the center of the dielectric structure. Therefore, they induce a dipolar effect when the bunch trajectory is not aligned to the longitudinal axis of the structure [13–18]. The transverse wake potential is calculated as the convolution of the transverse wake function w (depending on the geometry, the dielectric material and the bunch transverse offset with respect to the center of the structure) with the longitudinal charge density distribution of the bunch $n_b(t)$.

Thus, when a bunch travels with transverse offset (x, y), parallel to its axis, it drives transverse dipolar wakefields along the bunch described by [16]: $W_\perp(t) = w(x, y) \int_0^t n_b(t) dt$, where the bunch front is at $t = 0$. The amplitude of the wakefields follows the same trend as the running integral of the bunch charge: particles in the back of the bunch are deflected more strongly than those in the front. The polarity of $W_\perp$ is such that the trailing particles are pulled further toward the dielectric material [19].

Dielectric capillaries are common tools for generating plasmas in plasma wakefield accelerators (PWFA), as they enable gas injection in a high-vacuum environment [20]. The plasma is generated by ionizing the gas injected in the

capillary with a high-voltage discharge applied between electrodes at each end [21], or with an ionization field such as a high-intensity laser pulse [22] or a relativistic charged particle bunch [23]. Capillaries are also employed because they allow shaping the transverse and longitudinal profiles of the plasma density [24], and locally injecting different gas species for various injection schemes [25].

In a PWFA based on dielectric capillaries, both plasma and dielectric wakefields can be present at the same time, as the space-charge electric field of the driver bunch may interact with both plasma and dielectric material [26,27]. In particular, the possible misalignment of the trajectory with respect to the capillary longitudinal axis (e.g., due to jitters or to the finite accuracy of the alignment tools) may induce a deflection to the bunch trajectory. This could have detrimental effects on the propagation of the bunches and the acceleration quality, by inducing transverse phenomena such as beam breakup and hosing instability [28,29]. However, we show in the present work that high-density plasma suppresses the dielectric wakefields driven in the capillary, by screening the space-charge field of the bunch.

Experimental setup.—We performed the measurements at the SPARC_LAB facility [30] (see Fig. 1). An electron (e^-) bunch is generated by illuminating a copper cathode within a radiofrequency (RF) gun with an ultraviolet laser pulse. The bunch is accelerated in an RF linac to $E \sim 80$ MeV and focused with transverse root mean square (rms) radius $\sim$0.4 mm at the entrance of a dielectric capillary. A set of electromagnetic quadrupoles focuses the bunch on a scintillating screen $d = 5.3$ m downstream of the capillary exit for imaging. A transverse deflection structure (TDS) introduces a head-to-tail vertical correlation to the bunch [31], allowing one to obtain time-resolved images of the bunch at the screen position. The normalized emittance of the bunch is $\sim$2.4 μm (measured with quadrupole scan technique) and rms duration $\sim$1.8 ps. We use a magnetic dipole and an additional scintillating screen to measure the beam energy.

The dielectric capillary has radius $R_c = 1$ mm and length $L = 10$ cm. The plasma is generated by a discharge pulse ($\sim$455 A peak current) flowing through the capillary after the introduction of hydrogen gas ($\sim$10 mbar) through a high-speed solenoid valve. The capillary is installed in a vacuum chamber connected to the linac with a windowless,
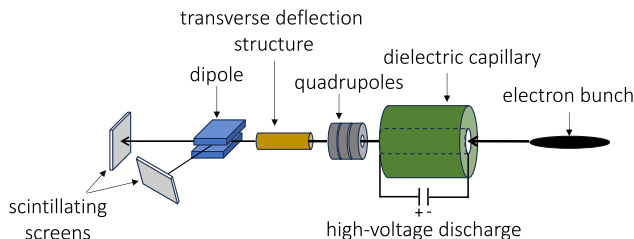

FIG. 1. Schematic of the SPARC_LAB experimental setup (not to scale). The e^- bunch propagates from right to left.

three-stage differential pumping system. The latter ensures that 10^{-8} mbar is maintained in the linac, while flowing the gas, and to preserve the quality of the electron bunch. By varying the delay between the bunch arrival time and the peak of the discharge pulse we vary n_{PE}, due to recombination of the plasma. We measure the average n_{PE} with the Stark broadening technique [32] between 0.65 and 2.65 μs after the peak of the discharge pulse, and we extrapolate the values of n_{PE} (with $\sim$10% uncertainty) at the delays used in the experiment (between 5.60 and 10.10 μs) by fitting the measured values with an exponential decay function [33]. The plasma electron density is essentially constant along the capillary (see Supplemental Material [34]), but nonuniformities are present at the two extremes because the gas flow expands in the vacuum chamber. However, as no capillary material is present, there is also no dielectric wakefield effect along the entrance and exit ramps. Thus, in the following we neglect these nonuniformities.

Current discharge is particularly suited for generating plasma in our experimental conditions because the moderate energy and current of the e^- bunch are not sufficient to field ionize hydrogen gas. Moreover, it is preferable over ionization with a laser pulse because it generates an almost uniform transverse plasma density profile, and it requires simpler synchronization and spatial alignment methods.

In the following, we maintain the beam trajectory aligned through the center of the quadrupole magnets, and we record images on the screen with the TDS turned on, and the dipole turned off. To study the effect of dielectric wakefields and plasma screening, we shift the capillary with a stepper motor in the horizontal direction (perpendicular to the streaking direction of the TDS, see Supplemental Material [34]), and we measure the induced deflection along the bunch on time-resolved images while varying the plasma electron density and, therefore, the plasma skin depth.

Experimental results.—Figure 2 shows single-event, time-resolved images of a 285 pC e^- bunch after traveling along the longitudinal axis of the dielectric capillary (a), and with a horizontal offset $X = 0.375$ mm (b). The bunch propagates from right to left (bunch front at $t = 0$). The red points show the centroid position along the bunch, obtained by fitting the transverse projection of each longitudinal slice with a Gaussian function. In the aligned case, the centroid position is essentially constant along the bunch, and the variations are much smaller than the bunch transverse size. The average centroid position obtained from 100 consecutive images (red points, left-hand-side vertical axis in Fig. 2(c); the error bars represent the standard deviation) is not correlated with the running sum of the bunch charge (black line, right-hand-side vertical axis; the shaded area is the standard deviation) because $w(0, 0) = 0$.

In the misaligned case [Fig. 2(b)], on the contrary, the centroid is clearly deflected, with increasing displacement along the bunch. Figure 2(d) shows that the centroid position and the running sum follow the same trend along
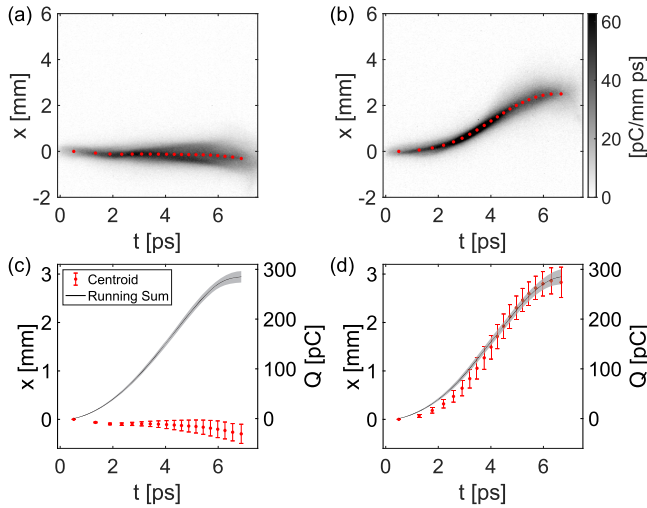
FIG. 2. (a), (b) Single-event, time-resolved images of the 285 pC e^- bunch for $X = 0$ (aligned case) and $X = 0.375$ mm, respectively. The bunch propagates from right to left. Red points indicate the centroid position of each longitudinal slice. (c), (d) Average centroid position along the bunch obtained from 100 consecutive events (red points, left-hand-side vertical axis; error bars are the standard deviation), corresponding to (a) and (b), respectively. Each black line shows the average running sum of the charge along the bunch (right-hand-side vertical axis, the shaded area represents the standard deviation).

FIG. 3. (a), (b) Single-event, time-resolved images of the e^- bunch with $X = 0.375$ mm [as in Fig. 2(b)], and plasma with $n_{PE} = 1.0$ and 0.038×10^{16} cm^{-3}, respectively. (c) Average centroid position along the bunch for $X = 0$ and $n_{PE} = 0$ (blue points), $X = 0.375$ mm and $n_{PE} = 0$ (black points), $n_{PE} = 0.038 \times 10^{16}$ cm^{-3} (red points) and $n_{PE} = 10^{16}$ cm^{-3} (green points).

the bunch. This confirms the expectation that the amplitude of the transverse wakefields (and therefore of the transverse deflection) at any time t along the bunch depends on the amount of charge ahead of it, in agreement with the formulation of $W_\perp(t)$.

The amplitude of the transverse wakefields $W_\perp$ reaches a maximum at the back of the bunch. We calculate the average wakefield potential experienced by the particles in the last slice of the bunch ($t \sim 6.7$ ps) as $W_\perp = x(t)E/edL \sim 0.4$ MV/m. We also note that, in both cases, the transverse size slightly increases along the bunch. This is due to the fact that the dielectric wakefields also have a quadrupolar (defocusing) component, growing in amplitude along the bunch.

When introducing plasma with $n_{PE} = 1.0 \times 10^{16}$ cm^{-3} while $X = 0.375$ mm [Fig. 3(a), same misalignment as Fig. 2(b)], the dielectric wakefields are suppressed because the plasma effectively screens the space-charge field of the bunch, since the plasma skin depth $\delta = 0.053$ mm is much shorter than the distance between the bunch and the dielectric surface $R_c - X = 0.625$ mm. Thus, the average position of the centroid along the bunch [green points in (c)] is in agreement with the aligned case with no plasma in the capillary [blue points, same dataset as Fig. 2(c)].

Slices at $t > 3$ ps have a wider transverse distribution because the bunch also drives plasma wakefields, that are axis symmetric with respect to the bunch propagation axis.
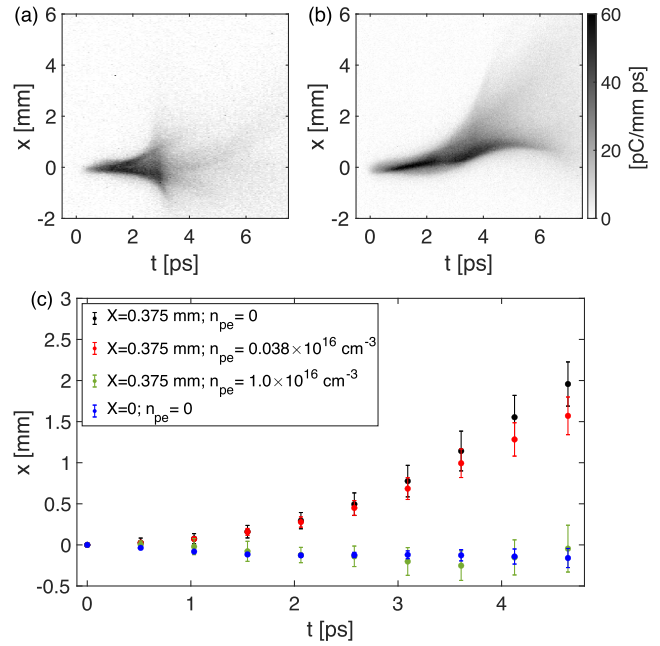
Additionally, the bunch self-focuses due to the effect of the magnetic field generated by the bunch current itself, that is not compensated for by the space-charge force, which is neutralized by the plasma [37–39]. As the bunch is progressively focused, it leaves the plasma with increasing divergence along the bunch, and possibly larger emittance, causing the transverse size to increase at the downstream screen. Because of this effect, we calculate the position of the centroid only for $t < 4.6$ ps.

On the contrary, when $n_{PE} = 0.038 \times 10^{16}$ cm^{-3} [Fig. 3(b)], plasma screening is not effective. In this case, $\delta = 0.237$ mm is not short enough to operate full screening, and the space-charge field of the bunch still reaches the dielectric surface, generating dielectric wakefields that affect the trajectory of the trailing part of the bunch. Thus, the horizontal position of the centroid along the bunch [red points in Fig. 3(c)] varies, in agreement with the case with no plasma [black points, same dataset as Fig. 2(d)]. We note that, in this case, dielectric wakefields (causing the centroid deflection) and plasma wakefields (causing the defocusing effect at the screen) are present at the same time.

Increasing n_{PE} decreases the distance from the propagation axis beyond which the space-charge field of the bunch is screened. Thus, for a small misalignment of the bunch trajectory with respect to the center of the dielectric capillary (i.e., a large distance from the surface), a lower n_{PE} is sufficient to suppress the dielectric
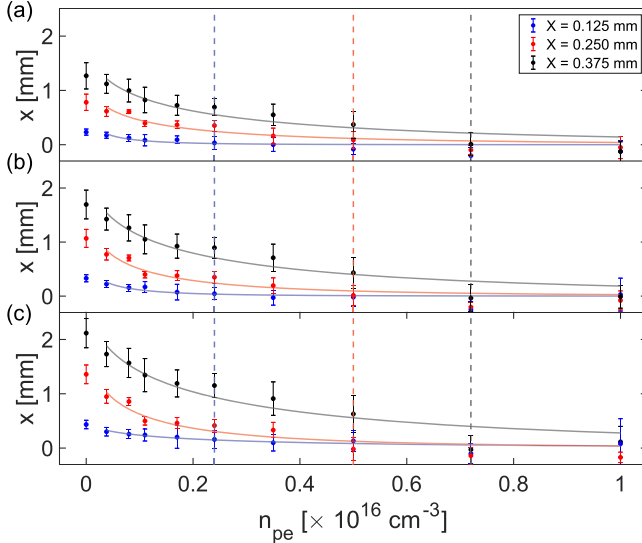
FIG. 4. Average centroid position x as a function of n_{PE} for three misalignment distances at longitudinal slices $t = 3.6$ ps (a), 4.1 ps (b), 4.6 ps (c) behind the front of the bunch. Dashed vertical lines indicate the values of n_{PE} after which x is in agreement with the aligned case with no plasma, for each misalignment distance.

wakefields than for a large misalignment (i.e., a short distance from the surface).

Figure 4 shows the position of the centroid at $t = 3.6$ ps (a), 4.1 ps (b), and 4.6 ps (c) behind the front of the bunch as a function of n_{PE}, for three misalignment distances (see Legend). The displacement, which is due to the effect of the dielectric wakefields, decreases when increasing n_{PE} because the amplitude of the space-charge field reaching the dielectric surface is progressively more screened by plasma. The trend is in good agreement with the typical exponential decay expected from plasma screening. The solid lines show the result of the fit for each dataset, where the distance from the bunch to the dielectric surface is considered as a free parameter.

For $X = 0.375$ mm (black points), full screening (i.e., centroid position in agreement with the aligned case with no plasma) occurs for $n_{PE} > 0.7 \times 10^{16}$ cm^{-3} (black dashed vertical line), corresponding to $\delta < 0.063$ mm, that is ~10 times shorter than the distance between the bunch and capillary surface $R_c - X = 0.625$ mm. For smaller misalignments, screening occurs at lower n_{PE}: for $R_c - X = 0.750$ mm, $n_{PE} > 0.5 \times 10^{16}$ cm^{-3} ($\delta < 0.075$ mm, red points and dashed vertical line); and for $R_c - X = 0.875$ mm, $n_{PE} > 0.24 \times 10^{16}$ cm^{-3} ($\delta < 0.109$ mm, blue points and dashed vertical line). As expected from the screening process, δ must be much shorter than the distance between the bunch and dielectric surface to obtain full screening. We also note that the ratio $(R_c - X)/\delta$ at full screening increases when the misalignment increases. This is likely due to the finite transverse size of the bunch,

as some particles are closer to the dielectric material than those at the bunch center.

As the bunch travels in plasma, it can drive plasma wakefields that also have a transverse (periodically focusing or defocusing) component [6,7], generally growing along the bunch [see Figs. 3(a) and 3(b)]. However, the fact that the transition to full screening occurs at the same n_{PE} for all delays along the bunch, as highlighted by the vertical lines in Fig. 4, indicates that the screening of the space-charge field is independent of the amplitude of the plasma wakefields. The displacement is larger for larger misalignments, at any t along the bunch where the plasma screening is not fully effective because $w(x, y)$ increases.

The experimental evidence we present in this work will have significant implications for designing and operating plasma-based accelerators. In particular, the direct observation of space-charge screening in plasma could be employed for managing misalignments and optimizing plasma conditions to minimize undesired wakefield effect.

Considering future PWFA, the operational n_{PE} and the transverse size of the capillary must be chosen so that the dielectric wakefields induced by misalignments (e.g., caused by jitters and finite accuracy of the alignment tools) are effectively screened by the plasma. In the case of EuPRAXIA@SPARC_LAB [40], the diameter of the dielectric capillary will be 2 mm, and the operational density $n_{PE} = 10^{16}$ cm^{-3}. The maximum misalignment allowed to avoid the dielectric wakefields effect would therefore be even larger than $X = 0.375$ mm, as shown in this study, which is much larger than the state-of-the-art capabilities to align and control the trajectory of relativistic particle bunches (e.g., better than 20 μm in our experiment). The measurement we present in this work could also be extended to a plasma electron density diagnostics, by measuring the maximum misalignment for which full screening of the space-charge field occurs.

Summary.—We investigated, with a noninvasive measurement, one of the fundamental characteristics of plasma, that is the screening of electromagnetic fields. We showed, using a plasma wakefield accelerator based on a dielectric capillary, that plasma screens the space-charge field of a relativistic e^- bunch by measuring the suppression of dielectric wakefields. The effect of transverse dielectric wakefields increases along the bunch, following the same trend as the running sum of the bunch charge, in agreement with the theory. We observed a progressively increasing screening effect when increasing the plasma electron density, and therefore decreasing the plasma skin depth. We measured full screening to occur along the entire bunch when the distance from the bunch propagation axis to the dielectric surface is more than 10 times longer than the plasma skin depth. When full screening is not achieved, dielectric and plasma wakefields are present simultaneously. We also discussed the implications for future plasma-based accelerators based on dielectric capillaries.

---

[*]Contact author: livio.verra@lnf.infn.it

[1] F. F. Chen, *Introduction to Plasma Physics and Controlled Fusion* (Springer International Publishing, New York, 2016).

[2] F. Otsuka, T. Hada, S. Shinohara, and T. Tanikawa, Penetration of a radio frequency electromagnetic field into a magnetized plasma: One-dimensional pic simulation studies, Earth Planets Space **67**, 85 (2015).

[3] S. Shinohara and K. P. Shamrai, Effect of electrostatic waves on a rf field penetration into highly collisional helicon plasmas, Thin Solid Films **407**, 215 (2002).

[4] T. Shoji, Description of radio-frequency plugging and heating in terms of plasma impedance, J. Phys. Soc. Jpn. **49**, 327 (1980).

[5] D. A. Whelan and R. L. Stenzel, Electromagnetic-wave excitation in a large laboratory beam-plasma system, Phys. Rev. Lett. **47**, 95 (1981).

[6] P. Chen, J. M. Dawson, R. W. Huff, and T. Katsouleas, Acceleration of electrons by the interaction of a bunched electron beam with a plasma, Phys. Rev. Lett. **54**, 693 (1985).

[7] R. Keinigs and M. E. Jones, Two-dimensional dynamics of the plasma wakefield accelerator, Phys. Fluids **30**, 252 (1987).

[8] J. D. Jackson, *Classical Electrodynamics* (John Wiley & Sons, New York, 1962).

[9] K. L. Bane, P. B. Wilson, and T. Weiland, Wake fields and wake field acceleration, AIP Conf. Proc. **127**, 875 (1985).

[10] W. Gai, P. Schoessow, B. Cole, R. Konecny, J. Norem, J. Rosenzweig, and J. Simpson, Experimental demonstration of wake-field effects in dielectric structures, Phys. Rev. Lett. **61**, 2756 (1988).

[11] R. Keinigs, W. Peter, and M. E. Jones, A comparison of the dielectric and plasma wakefield accelerators, Phys. Fluids B **1**, 1872 (1989).

[12] K.-Y. Ng, Wake fields in a dielectric-lined waveguide, Phys. Rev. D **42**, 1819 (1990).

[13] S. Y. Park and J. L. Hirshfield, Theory of wakefields in a dielectric-lined waveguide, Phys. Rev. E **62**, 1266 (2000).

[14] S. S. Baturin and A. D. Kanareykin, Cherenkov radiation from short relativistic bunches: General approach, Phys. Rev. Lett. **113**, 214801 (2014).

[15] S. Bettoni, P. Craievich, A. A. Lutman, and M. Pedrozzi, Temporal profile measurements of relativistic electron bunch based on wakefield generation, Phys. Rev. Accel. Beams **19**, 021304 (2016).

[16] P. Craievich and A. A. Lutman, Effects of the quadrupole wakefields in a passive streaker, Nucl. Instrum. Methods Phys. Res., Sect. A **865**, 55 (2017).

[17] B. D. O'Shea, G. Andonian, S. S. Baturin, C. I. Clarke, P. D. Hoang, M. J. Hogan, B. Naranjo, O. B. Williams, V. Yakimenko, and J. B. Rosenzweig, Suppression of deflecting forces in planar-symmetric dielectric wakefield accelerating structures with elliptical bunches, Phys. Rev. Lett. **124**, 104801 (2020).

[18] Y. Saveliev, T. J. Overton, T. H. Pacey, N. Joshi, S. Mathisen, B. D. Muratori, N. Thompson, M. P. King, and G. Xia, Experimental study of transverse effects in planar dielectric wakefield accelerating structures with elliptical beams, Phys. Rev. Accel. Beams **25**, 081302 (2022).

[19] A. W. Chao, *Physics of Collective Beam Instabilities in High-Energy Accelerators* (John Wiley & Sons, Inc., New York, 1993).

[20] W. P. Leemans, B. Nagler, A. J. Gonsalves, C. Tóth, K. Nakamura, C. G. R. Geddes, E. Esarey, C. B. Schroeder, and S. M. Hooker, GeV electron beams from a centimetre-scale accelerator, Nat. Phys. **2**, 696 (2006).

[21] D. J. Spence and S. M. Hooker, Investigation of a hydrogen plasma waveguide, Phys. Rev. E **63**, 015401 (2000).

[22] L. V. Keldysh, Ionization in the field of a strong electromagnetic wave, J. Exp. Theor. Phys. **20**, 1307 (1965).

[23] C. L. O'Connell, C. D. Barnes, F.-J. Decker, M. J. Hogan, R. Iverson, P. Krejcik, R. Siemann, D. R. Walz, C. E. Clayton, C. Huang, D. K. Johnson, C. Joshi, W. Lu, K. A. Marsh, W. Mori, M. Zhou, S. Deng, T. Katsouleas, P. Muggli, and E. Oz, Plasma production via field ionization, Phys. Rev. ST Accel. Beams **9**, 101301 (2006).

[24] W. P. Leemans, A. J. Gonsalves, H.-S. Mao, K. Nakamura, C. Benedetti, C. B. Schroeder, C. Tóth, J. Daniels, D. E. Mittelberger, S. S. Bulanov, J.-L. Vay, C. G. R. Geddes, and E. Esarey, Multi-GeV electron beams from capillary-discharge-guided subpetawatt laser pulses in the self-trapping regime, Phys. Rev. Lett. **113**, 245002 (2014).

[25] M. Chen, E. Esarey, C. B. Schroeder, C. G. R. Geddes, and W. P. Leemans, Theory of ionization-induced trapping in laser-plasma accelerators, Phys. Plasmas **19**, 033101 (2012).

[26] C. T. C. Li and H. Zha, Calculation of wakefield in plasma-filled dielectric capillaries generated by a relativistic electron beam, in *Proceedings of the IPAC'13* (JACoW Publishing, Geneva, Switzerland, 2013).

[27] A. Biagioni, M. Anania, M. Bellaveglia, E. Brentegani, G. Castorina, E. Chiadroni, A. Cianchi, D. Di Giovenale, G. Di Pirro, H. Fares, L. Ficcadenti, F. Filippi, M. Ferrario, A. Mostacci, R. Pompili, J. Scifo, B. Spataro, C. Vaccarezza, F. Villa, and A. Zigler, Wake fields effects in dielectric capillary, Nucl. Instrum. Methods Phys. Res., Sect. A **909**, 247 (2018).

[28] D. H. Whittum, W. M. Sharp, S. S. Yu, M. Lampe, and G. Joyce, Electron-hose instability in the ion-focused regime, Phys. Rev. Lett. **67**, 991 (1991).

[29] T. Nechaeva *et al.* (AWAKE Collaboration), Hosing of a long relativistic particle bunch in plasma, Phys. Rev. Lett. **132**, 075001 (2024).

[30] M. Ferrario *et al.*, SPARC_LAB present and future, Nucl. Instrum. Methods Phys. Res., Sect. B **309**, 183 (2013).

[31] D. Alesini, G. Di Pirro, L. Ficcadenti, A. Mostacci, L. Palumbo, J. Rosenzweig, and C. Vaccarezza, Rf deflector

design and measurements for the longitudinal and transverse phase space characterization at sparc, Nucl. Instrum. Methods Phys. Res., Sect. A **568**, 488 (2006).

[32] M. Qian, C. Ren, D. Wang, J. Zhang, and G. Wei, Stark broadening measurement of the electron density in an atmospheric pressure argon plasma jet with double-power electrodes, J. Appl. Phys. **107**, 063303 (2010).

[33] V. Shpakov *et al.*, Longitudinal phase-space manipulation with beam-driven plasma wakefields, Phys. Rev. Lett. **122**, 114801 (2019).

[34] See Supplemental Material at http://link.aps.org/supplemental/10.1103/PhysRevLett.133.035001 for details on the experimental setup, which includes Refs. [35,36].

[35] A. Biagioni, M. P. Anania, S. Arjmand, E. Behar, G. Costa, A. D. Dotto, M. Ferrario, M. Galletti, V. Lollo, D. Pellegrini, G. D. Pirro, R. Pompili, Y. Raz, G. Russo, and A. Zigler, Gas-filled capillary-discharge stabilization for plasma-based

accelerators by means of a laser pulse, Plasma Phys. Controlled Fusion **63**, 115013 (2021).

[36] M. Galletti, M. P. Anania, S. Arjmand, A. Biagioni, G. Costa, M. Del Giorno, M. Ferrario, V. Lollo, R. Pompili, Y. Raz, V. Shpakov, F. Villa, A. Zigler, and A. Cianchi, Advanced stabilization methods of plasma devices for plasma-based acceleration, Symmetry **14**, 450 (2022).

[37] P. Chen, A possible final focusing mechanism for linear colliders, Part. Accel. **20**, 171 (1987).

[38] N. Barov and J. B. Rosenzweig, Propagation of short electron pulses in underdense plasmas, Phys. Rev. E **49**, 4407 (1994).

[39] L. Verra, E. Gschwendtner, and P. Muggli, Focusing of a long relativistic proton bunch in underdense plasma, *Proceedings of the 2022 IEEE Advanced Accelerator Concepts Workshop (AAC)* (2023); arXiv:2302.04051.

[40] R. W. Assmann *et al.*, Eupraxia conceptual design report, Eur. Phys. J. Spec. Top. **229**, 3675 (2020).